Density-of-states-driven transition from superconductivity to ferromagnetism in Ce(Ru$_{1-x}$Rh$_x$)$_3$B$_2$: Scenario for an exchange-split Kondo resonance

J. W. Allen

Department of Physics, University of Michigan, Ann Arbor, Michigan 48109-1120

M. B. Maple, J.-S. Kang,* and K. N. Yang

*Department of Physics and Institute for Pure and Applied Physical Sciences,
University of California at San Diego, La Jolla, California 92093*

M. S. Torikachvili

Department of Physics, San Diego State University, San Diego, California 92182

Y. Lassailly

Ecole Polytechnique, 91128 Palaiseau, France

W. P. Ellis

Los Alamos National Laboratory, Los Alamos, New Mexico 87545

B. B. Pate and I. Lindau

Stanford Synchrotron Radiation Laboratory, Stanford, California 94305
(Received 23 October 1989)

We have investigated the interesting alloy system Ce(Ru$_{1-x}$Rh$_x$)$_3$B$_2$, where the physical properties change from superconducting to ferromagnetic as x changes from 0 to 1. We report the results of transport, magnetic, crystallographic, and electron-spectroscopy measurements, and a theoretical analysis of the electron-spectroscopy data using the impurity Anderson Hamiltonian applied to the Ce $4f$ electrons. Superconductivity exists in the range $0 < x < 0.38$, while ferromagnetism occurs in the range $0.84 < x < 1$. Our studies of superconductivity and ferromagnetism in Ce(Ru$_{1-x}$Rh$_x$)$_3$B$_2$ show that ferromagnetism is associated with nearly trivalent Ce ions. We find that the alloying mechanism controlling the low-energy properties of this system is the transition-metal $4d$ density of states at the Fermi level, rather than any parameter directly connected to the $4f$ states, such as its binding energy, Coulomb interaction, or the average hybridization strength between the localized $4f$ and conduction electrons. We use this result to further elucidate our previously proposed exchange split-Kondo resonance model of the ferromagnetism near $x = 1$.

I. INTRODUCTION

An important component of the recent activity in the field of heavy fermions and intermediate valence is the discovery of new materials with novel properties. Among the most intriguing are alloy systems in which dramatic changes in ground-state properties occur with apparently modest or even trivial changes in chemical composition. It has generally been the case that the microscopic origins of this alloy behavior are not understood and the development of these materials depends largely on intuition rooted in a knowledge of empirical trends. Measurements of spectroscopic properties, correlated with a knowledge of ground-state properties, offer the possibility of elucidating the microscopic origins of alloying behavior. This paper describes such a study for the alloy system Ce(Ru$_{1-x}$Rh$_x$)$_3$B$_2$.

The motivation for this work springs from the properties of compounds of the type CeT_3B$_2$,[1] with $T = $ Ir, Rh, and Ru, which exhibit a variety of phenomena; CeRh$_3$B$_2$ is ferromagnetic,[1,2] CeIr$_3$B$_2$ displays typical valence fluctuation anomalies in its physical properties,[1] and CeRu$_3$B$_2$ becomes superconducting at 0.68 K.[1] All of the compounds have reduced unit-cell volumes,[1,3] indicating that the Ce ions have a valence intermediate between 3 + and 4 +. Early work on polycrystalline samples of CeRh$_3$B$_2$ established that its ferromagnetism is rather unusual in several respects. This work found a relatively high Curie temperature $T_M \approx 113$ K,[1,2] in contrast with the behavior of most metallic compounds of Ce with nonmagnetic elements, which are antiferromagnets with low Néel temperatures in the range of 10 K.[4] This Curie temperature is much higher than the value $T_M \approx 1$ K, expected by assuming that the magnetic ordering involves Ce^{3+} localized moments and by applying a simple de Gennes scaling of the Curie temperature of GdRh$_3$B$_2$ ($T_M \approx 90$ K) to CeRh$_3$B$_2$. This work also found an effective magnetic moment $\mu_{\text{eff}} = 1\mu_B$/Ce ion[1,5] and a saturation moment at low temperature $\mu_s = 0.38\mu_B$/Ce ion,[1,2,5] which are substantially reduced with respect to the Ce^{3+} free-

ion values $\mu_{eff} = 2.54\mu_B$ with $\mu_s = 2.15\mu_B$. This moment reduction cannot be accounted for by the hexagonal crystal-field effect which splits the ground-state multiplet $J = \frac{5}{2}$ into three doublets.[6,7] As discussed further below, these and other results have motivated explanations of the ferromagnetism which draw on both localized and itinerant models of magnetism, and this basic conflict is not yet resolved.

To understand the origin of the unusual ferromagnetism of $CeRh_3B_2$, and to search for interesting effects arising from the interplay between superconductivity and ferromagnetism, we have investigated polycrystalline samples of the pseudoternary system $Ce(Ru_{1-x}Rh_x)_3B_2$, using transport, magnetic, crystallographic, and electron-spectroscopy measurements. In this paper we report x-ray diffraction data, the ac and dc magnetic susceptibility, and the electrical resistivity for many values of x. For $x = 0$, 0.2, and 1, we report the spectra obtained from Ce $3d$ x-ray photoemission spectroscopy (XPS), from Ce $4f$ resonant photoemission spectroscopy (RESPES), and from Ce $4f$ bremsstrahlung isochromat spectroscopy (BIS). Our transport, magnetic, and crystallographic studies[1,8,9] were carried out independently of, and at about the same time as, the work of Shaheen *et al.*[10] The spectroscopic work was begun at this time also. We have previously published[8] some of the transport data, the RESPES spectra for $x = 0$ and 1, and a suggestion that the ferromagnetism of $CeRh_3B_2$ be modeled in terms of an exchange-split Kondo resonance. The RESPES spectrum for $x = 1$ agreed with that obtained at about the same time by Sampathkumaran *et al.*[11] The BIS data, the RESPES data for $x = 0.2$, and the Ce $3d$ XPS data for $x = 0$ and 0.2, are new, although the Ce $3d$ XPS spectrum for a single-crystal sample with $x = 1$ was recently reported by Kasaya *et al.*[12] Also new in this paper are the results of an analysis of all the spectra using the impurity Anderson Hamiltonian.

Our studies show that superconductivity exists in the range $0 < x < 0.38$, while ferromagnetism occurs in the range $0.84 < x < 1.0$, and that ferromagnetism is associated with nearly trivalent Ce ions. We find that the alloying mechanism which controls the low-energy properties of this system is the transition-metal $4d$ density of states at the Fermi level, rather than any parameter directly connected to the $4f$ state, such as its binding energy, Coulomb interaction, or the average hybridization strength between localized $4f$ and conduction electrons. We use this result to discuss the alloy system in terms of a Kondo Fermi liquid and to further elucidate how our exchange-split Kondo resonance model[8] applies to the ferromagnetism of $CeRh_3B_2$. The organization of this paper is as follows: Section II describes experimental details, Sec. III reports transport measurements, Sec. IV reports the impurity Anderson Hamiltonian analysis of the Ce $3d$ XPS and $4f$ PES/BIS data, Sec. V gives a discussion of the results and of the ferromagnetism of $CeRh_3B_2$, and Sec. VI summarizes our conclusion.

II. EXPERIMENTAL DETAILS

All the samples studied in this paper were polycrystalline samples. They were prepared by arc melting high-purity elements (99.9% pure Ce, Ru, and Rh; 99.9995% pure B) in a Zr-gettered argon atmosphere followed by annealing in argon at 900 °C for 14 d. Portions of the samples were powdered and analyzed by x-ray diffraction to determine the crystal structure and lattice parameters. The diffraction patterns of $Ce(Ru_{1-x}Rh_x)_3B_2$ samples could be indexed to the hexagonal $CeCo_3B_2$ crystal structure ($P6/mmm$) to within an accuracy in diffraction angle $\Delta 2\theta$ of $\pm 0.15°$ and did not indicate the presence of any impurity phases to within the limit of detectability ($< 5\%$). The $CeCo_3B_2$ crystal structure contains one formula unit per unit cell and is derived from the binary $CaCu_5$-type crystal structure, in which the Cu atoms occupy two different crystallographic sites.

Electrical resistivity ρ measurements were made with a standard four-lead ac technique at a frequency of 16 Hz in the temperature range $1 < T < 300$ K. The ac magnetic susceptibility χ_{ac} was measured with a mutual inductance technique at 16 Hz in the earth's magnetic field for 80 mK $< T < 6$ K. Magnetization measurements were carried out in an SHE superconducting quantum interference device (SQUID) magnetometer in magnetic fields up to 40 kOe for $2 < T < 300$ K.

RESPES measurements were performed at the Stanford Synchrotron Radiation Laboratory (SSRL) using monochromatic photons obtained from the grasshopper monochromators on beam lines I-1 and III-1. A commercial double-pass cylindrical mirror analyzer was used to analyze the kinetic energies of the emitted electrons, and measured surfaces were obtained by fracturing samples *in situ* in an ultrahigh-vacuum chamber having a base pressure between $\sim 5 \times 10^{-11}$ Torr and $\sim 1 \times 10^{-10}$ Torr for various runs. The resolutions of the photon energy and electron kinetic energy combined give an experimental resolution of ~ 0.8 eV. The $Ce(Ru_{1-x}Rh_x)_3B_2$ sample temperatures were ~ 300 K for $x = 0$ and 1, and ~ 100 K for $x = 0.2$. The Fermi level of the system was determined from the valence-band spectrum of a gold sample evaporated onto a stainless steel substrate *in situ*. For normalization of the spectra, the photon flux was monitored by the yield from a stainless-steel target. BIS and XPS spectra were taken at a photon energy of 1486.6 eV in a Vacuum Generators ESCALAB at the Xerox Palo Alto Research Center. The XPS and BIS spectra were obtained from the same samples for which the RESPES data were obtained. The sample temperature during the XPS and BIS measurements was ~ 100 K. The Ce $3d$ core-level XPS data were obtained with a non-monochromatic Al $K\alpha$ source, yielding an overall resolution due to photon- and electron-energy resolutions of ~ 1.2 eV. Satellites due to the Al $K\alpha_{3,4}$ lines were removed from the spectra by a standard algorithm which we have demonstrated[13] to be reliable for Ce $3d$ spectra by comparison to spectra taken using a monochromatic Al $K\alpha$ source. The overall instrumental resolution for the BIS spectra is ~ 0.6 eV. The Fermi level of the system was determined from the valence- and conduction-band spectra of a silver sample cleaned by Ar-ion sputtering *in situ*. The inelastic backgrounds were subtracted in such a way[14] that the background at binding energy ε is proportional to the convolution of the primary spectrum

with the inelastic loss spectrum, which is approximated by a step function at ε. The inelastic background to the BIS spectra were removed by assuming a straight line.

The length of time that a sample surface remains free of oxygen and carbon after fracturing varies from sample to sample and is frequently less than the time to form a monolayer at the ambient pressure for a sticking coefficient of one. This suggests that the surface is contaminated by diffusion of oxygen or carbon along grain boundaries from the bulk to the surface. The diffusion of carbon seems to be faster during BIS measurements than during PES measurements, and we have found that this is not due to sample heating by controlling the sample temperature to be the same for both measurements. Diffusion of both oxygen and carbon is greatly slowed by cooling the sample to ~ 100 K, and this was done for the BIS-XPS measurements. As we discuss in Sec. IV, the valence bands of some of our samples have, even for freshly fractured surfaces, emission that we believe is due to grain-boundary carbon.

III. RESULTS OF TRANSPORT, MAGNETIC, AND CRYSTALLOGRAPHIC MEASUREMENTS

Figure 1 shows the curves of χ_{ac} versus T for four superconducting $Ce(Ru_{1-x}Rh_x)_3B_2$ compounds with $0.1 < x < 0.3$. The superconducting transition temperature T_c is defined as the temperature at which the decrease in χ_{ac} associated with the superconductivity attains 50% of its maximum value, while the superconducting transition width is determined from 10 to 90 % values of T_c. The values of T_c and its width versus x are plotted in Fig. 2. With increasing Rh concentration, T_c initially increases from 0.68 K at $x = 0$ to 0.81 K at $x = 0.1$, and then decreases nearly linearly with x between $x = 0.1$ and 0.3. A linear extrapolation T_c versus x above $x = 0.3$ yields $T_c = 0$ K at $x = 0.38$. A similar initial increase and subsequent decrease of T_c with x occurs in $(Ce_{1-x}R_x)Ru_2$ systems, where R represents a rare-earth element.[14] The slope of the linear region of the T_c versus x curve is
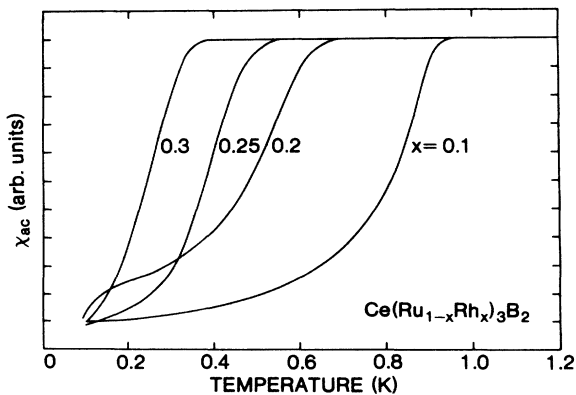

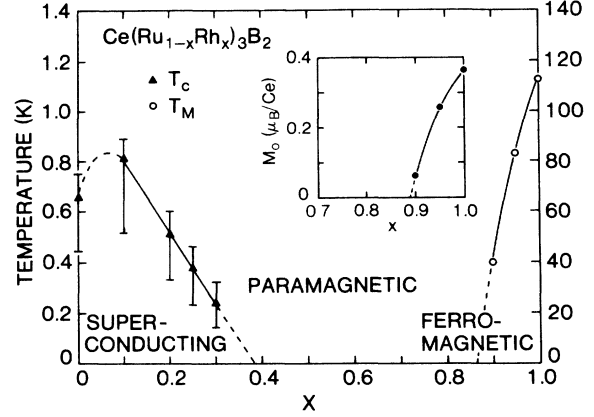
FIG. 2. Superconducting transition temperature T_c and Curie temperature T_M vs Rh concentration x for the $Ce(Ru_{1-x}Rh_x)_3B_2$ system.

equal to $\sim 2.9 \times 10^{-2}$ K/at. % Rh substitution for Ru. Shaheen et al.[10] reported a monotonic decrease of T_c with x in the related system $(La_{1-x}Ce_x)Rh_3B_2$ with an initial slope of -5.6 K/(at. % Ce substitution) for La.

Figure 3 shows plots of the lattice parameters a and c, the c/a ratio, and the unit-cell volume v versus x. With increasing Rh concentration, the lattice parameter a increases slightly, attains a maximum value at $x = 0.6$, and then decreases, while the lattice parameter c first decreases, exhibits a broad minimum at $x = 0.6$, and then
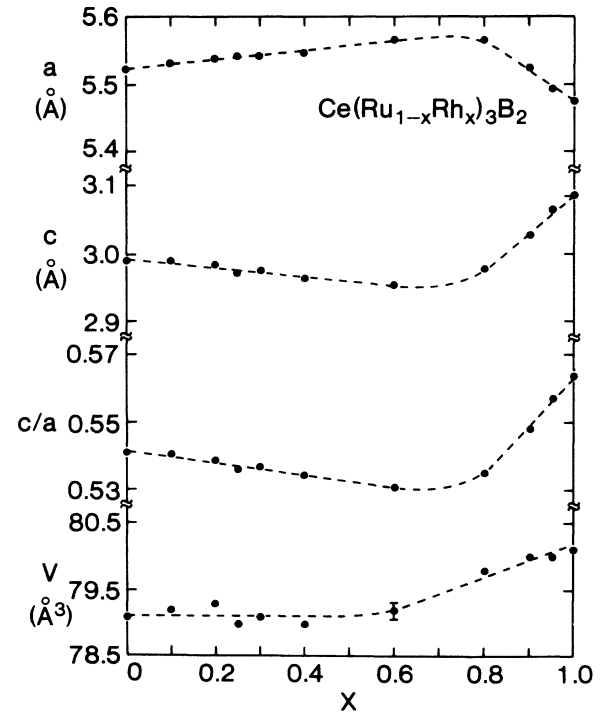

FIG. 1. The ac magnetic susceptibility χ_{ac} vs temperature superconducting transition curves for $Ce(Ru_{1-x}Rh_x)_3B_2$ compounds with $x = 0.1, 0.2, 0.25,$ and 0.3.

FIG. 3. Lattice parameters a and c, c/a ratio, and unit-cell volume v vs Rh concentration x for the $Ce(Ru_{1-x}Rh_x)_3B_2$ system. The error bar represents the typical uncertainty for all of the values of v.

increases. As a consequence, the unit-cell volume v is essentially constant between $x = 0$ and 0.6 and increases with x for $x > 0.6$. The variation of v with x is similar to that reported by Malik *et al.*[15]

Figure 4(a) shows the low-temperature magnetization M versus applied-magnetic-field H data for $Ce(Ru_{1-x}Rh_x)_3B_2$ ($x = 0.8, 0.9, 0.95$). For $x = 0.8$, the M versus H curve at 6 K is linear indicating that it is paramagnetic for $T > 6$ K; no magnetic transition could be detected in this sample by means of χ_{ac} measurements for $0.1 < T < 6$ K. For $x = 0.9$ and 0.95, linear extrapolations of the high-field M versus H data to $H = 0$ at various temperatures yield nonzero saturation moments $M_0(T)$; the values of M_0 at $T < 2$ K are depressed relative to the value for $x = 1$. For $x = 0.95$, $M_0(T = 1.7$ K) is $0.26\mu_B$/Ce ion, $\sim 70\%$ of the value for $x = 1$, while for $x = 0.9$, $M_0(T = 2$ K) is $0.062\mu_B$/Ce ion, only $\sim 17\%$ of the value for $x = 1$. Thus, the substitution of Ru for Rh in $CeRh_3B_2$ produces a nearly linear depression of μ_s with Ru concentration, $(1-x)$, at an initial rate of $\sim -0.03\mu_B$/Ce ion at. % Ru substitution for Rh, which extrapolates to $\mu_s = 0$ at $x = 0.88$.

Low-field ($H = 100$ G) M versus T data for $x = 0.9$ and 0.95 are shown in Fig. 4(b). The M versus T curves for both compounds reflect the transition to the ferromagnetic state. Linear extrapolation of M^2 versus T to $M = 0$ for both compounds yields estimates of the Curie temperature of $T_M = 40$ and 86 K for $x = 0.9$ and 0.95, respectively. Plots of M^2 versus (H/M) (Arrott plots) at temperatures in the vicinity of the Curie temperature for both of these compounds are shown in Fig. 5. Linear extrapolation of the high-field M^2 versus (H/M) data to $H = 0$ for $x = 0.5$ shows that $M^2(0)$ vanishes at $T_M = 83$ K, which is in good agreement with the value estimated from the low-field M versus T data [in Fig. 4(b)]. However, it is not possible to extract a value for T_M from M^2 versus (H/M) plots for the $x = 0.9$ compound, presumably because of a small value of μ_s and large Pauli paramagnetic susceptibility of the conduction electrons.
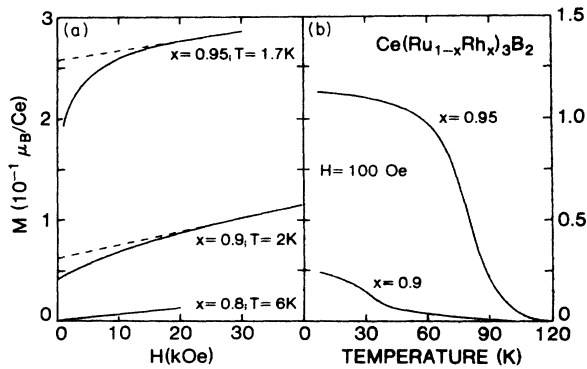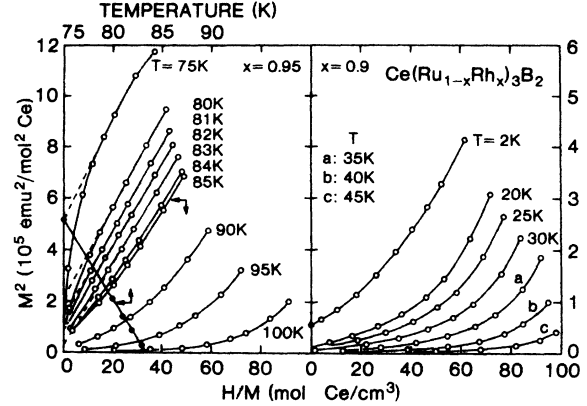
FIG. 5. M^2 vs H/M isotherms for two $Ce(Ru_{1-x}Rh_x)_3B_2$ compounds with $x = 0.9$ and 0.95. M is the magnetization and H is the applied magnetic field. Zero-field values of M^2, obtained by linear extrapolation of the high-field M^2 vs H/M data to $H = 0$, are plotted vs T for the compound with $x = 0.95$.

These results shown in Figs. 1–5 are summarized in Table I.

Open circles, in Fig. 6 and in the inset, show the magnetic susceptibility $\chi(T)$ and $\chi^{-1}(T)$ data, respectively, for $x = 0.8$. The upturn in $\chi(T)$ at low temperatures is probably caused by impurity phases. At temperatures below 30 K, the $\chi(T)$ data can be described by the expression

$$\chi(T) = \frac{C}{T - \Theta} + \chi_0 , \tag{1}$$

where the Curie-Weiss term, $C/(T - \Theta)$, is presumed to represent the impurity phase contribution. The values obtained by fitting the data to Eq. (1) are $C = 1.14 \times 10^{-2}$ cm^3 K/mol (one mole refers to a formula unit) and $\Theta = -1.8$ K. This value of C corresponds to 1.4 at. % Ce^{3+} free ions with an effective magnetic moment $\mu_{eff} = 2.54\mu_B$. The solid line in Fig. 6 represents the behavior of $\chi(T)$, after the impurity contribution has been

FIG. 4. (a) Low-temperature magnetic M vs applied magnetic field H isotherms for $Ce(Ru_{1-x}Rh_x)_3B_2$ compounds with $x = 0.8, 0.9$, and 0.95. (b) Low-field (100 G) magnetization M vs temperature curve for $Ce(Ru_{1-x}Rh_x)_3B_2$ compounds with $x = 0.9$ and 0.95.
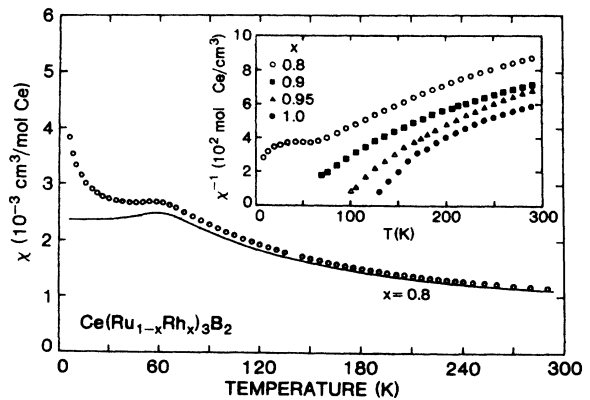
FIG. 6. Magnetization susceptibility χ vs temperature T and $\chi - 1$ vs T (inset) data for $Ce(Ru_{1-x}Rh_x)_3B_2$ compounds with $x = 0.8, 0.9, 0.95$, and 1.0.

TABLE I. The superconducting transition temperature T_c, Curie temperature T_M, lattice parameters a, c, c/a ratio, and unit-cell volume v of the compound $Ce(Ru_{1-x}Rh_x)_3B_2$ for various x.

x	T_c (K)	T_M (K)	M_0 (μ_B/Ce)	a (Å) ±0.1	c (Å) ±0.1	c/a	v (Å^3)
0[a]	0.68			5.527	2.991	0.541	79.1
0.1	0.81			5.532	2.990	0.541	79.2
0.2	0.51			5.539	2.984	0.539	79.3
0.25	0.375			5.542	2.971	0.536	79.0
0.3	0.24			5.542	2.975	0.537	79.1
0.4				5.547	2.963	0.534	79.0
0.6				5.565	2.953	0.531	79.2
0.8				5.564	2.977	0.535	79.8
0.9		40	0.06	5.524	3.027	0.548	80.0
0.95		83	0.26	5.493	3.064	0.557	80.0
1.0[b]		113	0.37	5.474	3.085	0.564	80.1

[a]Reference 1.
[b]References 1 and 2.

subtracted. The corrected $\chi(T)$ data exhibit a maximum at $T=60$ K and can be extrapolated to $\chi_0=2.4\times10^{-3}$ cm^3/mol as $T\rightarrow0$ K, which is much larger than the value of χ_0 for CeRu$_3$B$_2$ right above T_c ($\approx5\times10^{-4}$ cm^3/mol).[16] This behavior of $\chi(T)$ is reminiscent of many intermediate valence Ce compounds.

Also shown in the inset of Fig. 6 are $\chi^{-1}(T)$ data for $x=0.9$, 0.95, and 1. The temperature dependence of χ does not follow a Curie-Weiss law, which may be due to both a small Ce effective magnetic moment and a large weakly temperature-dependent Pauli background contribution. The data for $T>T_M$ for compounds with $x=0.9$, 0.95, and 1, can also be analyzed with Eq. (1), where the Curie-Weiss term is associated with an intrinsic ferromagnetism, rather than with any impurity phases. Least-squares fits of the data to Eq. (1) yield $C=0.17\times10^{-2}$ cm^3 K/mol ($\mu_{eff}=1.2\mu_B$/Ce ion), $\Theta=36$ K, and $\chi_0=7.4\times10^{-4}$ cm^3/mol for $x=0.9$; $C=0.15\times10^{-2}$ cm^3 K/mol ($\mu_{eff}=1.1\mu_B$/Ce ion), $\Theta=87$ K, and $\chi_0=7.5\times10^{-4}$ cm^3/mol for $x=0.95$; $C=0.127\times10^{-2}$ cm^3 K/mol ($\mu_{eff}=1.0\mu_B$/Ce ion), and $\chi_0=9.3\times10^{-4}$ cm^3/mol for $x=1$. The values of C and χ_0 for $x=0.9$ and 0.95 are comparable to those for $x=1$. The value of Θ for $x=0.9$ is comparable to the value of T_M estimated from the low-field $M(T)$ data.

The values of the Curie temperatures, T_M, of the Ce(Ru$_{1-x}$Ru$_x$)$_3$B$_2$ compounds with $x=1$, 0.95, and 0.9, which we take to be 113 K[1], 83 K, and 40 K, respectively, are plotted in Fig. 2. The substitution of Ru for Rh in CeRh$_3$B$_2$ results in a rapid and nearly linear suppression of T_M at a rate of -7.3 K/at. % Ru substitution for Rh. According to a linear extrapolation of the Curie temperature to zero, the ferromagnetism will vanish for $x<0.84$. The strong decrease of the saturation moment μ_s and the Curie temperature T_M with Ru substitution observed in the present work is in reasonable agreement with the findings of Shaheen et al.[10] who estimated the lower limit of x for ferromagnetic order to be 0.8.

Figure 7 shows the electrical resistivity $\rho(T)$ data for compounds with $0.1<x<0.95$. There is a rapid de-

crease in the resistivity of the ferromagnetic compounds for temperatures below the Curie temperature, which is manifested as a maximum in the derivative $d\rho/dT$ shown in the inset of Fig. 7. The maximum in $d\rho/dT$ occurs at $T\sim75\pm5$ K for $x=0.95$ and at $T\sim45\pm10$ K for $x=0.9$, in rough agreement with the values of the Curie temperature determined from the magnetization data. The resistivities of all of the compounds are large, which is consistent with strong scattering of conduction electrons and
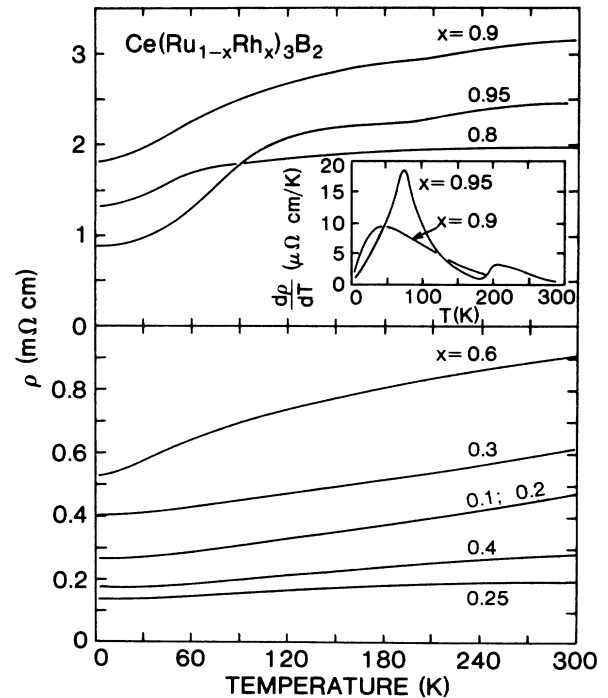

FIG. 7. Electrical resistivity ρ vs temperature T data for various Ce(Ru$_{1-x}$Rh$_x$)$_3$B$_2$ compounds with x between 0.1 and 0.95. Shown in the inset are $d\rho/dT$ vs T data for the samples with $x=0.9$ and 0.95.

microcrystalline imperfections in the samples, as previously noted for other CeT_3B_2 and UT_3B_2 compounds.[1]

IV. XPS-PES-BIS SPECTRA AND IMPURITY ANDERSON HAMILTONIAN ANALYSIS

In this section, we present our electron-spectroscopy data and an analysis of the data within the framework of the impurity Anderson Hamiltonian. The RESPES, BIS, and Ce $3d$ XPS measurements were made for $x = 0$, 0.2, and 1. Efforts to study a sample with $x = 0.8$ were frustrated by the fact that the grain structure is very loose for this composition so that the surfaces obtained by fracturing are not sufficiently clean. The points of Figs. 8 and 9 show, respectively, the Ce $3d$ spectra, and the $4f$ RESPES-BIS spectra. The solid lines show the theoretical analysis, discussed below. For $x = 1$, the surface obtained for the Ce $3d$ XPS and BIS measurements was slightly oxidized, and so we show in Fig. 8, and analyze below, the recently published single-crystal Ce $3d$ XPS spectrum[12] for $x = 1$. In Fig. 9, we show our BIS data for $x = 1$, even though it is slightly oxidized, because it helps to visualize the sequence of alloy spectra. The features in the BIS spectra near E_F and centered around 5 eV are due to $4f$ states and are discussed further below. The weaker structure centered at about 2 eV is often observed[13] in intermetallic compounds of rare earths and transition metals. In $CePd_3$ this structure has been

shown to arise from antibonding states formed by hybridization of the Pd $4d$ and rare-earth $5d$ states.[17] It is plausibly assigned analogously here. The photon energies of the RESPES measurements were chosen to take advantage of the Fano resonance[18] in the cross section for Ce $4f$ emission and of the Cooper minimum[19] in the cross section for Ru and Rh emission, in order to separate the various contributions to the valence-band spectrum. By happenstance, the energy range of the Cooper minimum for Ru and Rh includes the energies of the Ce $4f$ Fano minimum, 112 eV, and the Fano maximum, 122 eV. Thus, it is rather easy to extract the Ce $4f$ emission by subtracting the Fano minimum spectrum from the Fano maximum spectrum, with the result shown in Fig. 9.

Figure 10 shows the valence-band photoemission spectra for photon energy $h\nu = 80$ eV. For this photon energy, well below the Cooper minimum and the Fano maximum, the spectrum is dominated by Rh and Rh $4d$ emission[20] in the binding-energy range 0 to 6 eV. We have previously[8] drawn attention to the importance of the fact that as x changes from 0 to 1 the peak in the $4d$ states moves further below E_F. This reflects the larger nuclear charge of Rh, which binds an additional $4d$ electron and also differences in the extent to which $4d$ states are pushed below E_F by hybridization to Ce $5d$ states. The consequence is that the density of states at E_F falls with increasing x. In our Anderson Hamiltonian analysis below, this change is the most important factor in controlling the alloy behavior.
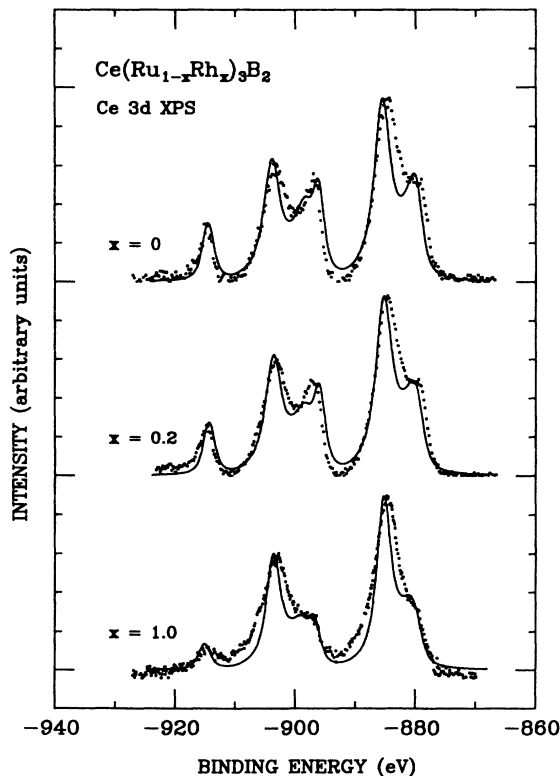

FIG. 8. The points and solid curves denote, respectively, the measured Ce $3d$ XPS spectra and the corresponding theoretical fits of $Ce(Ru_{1-x}Rh_x)_3B_2$.
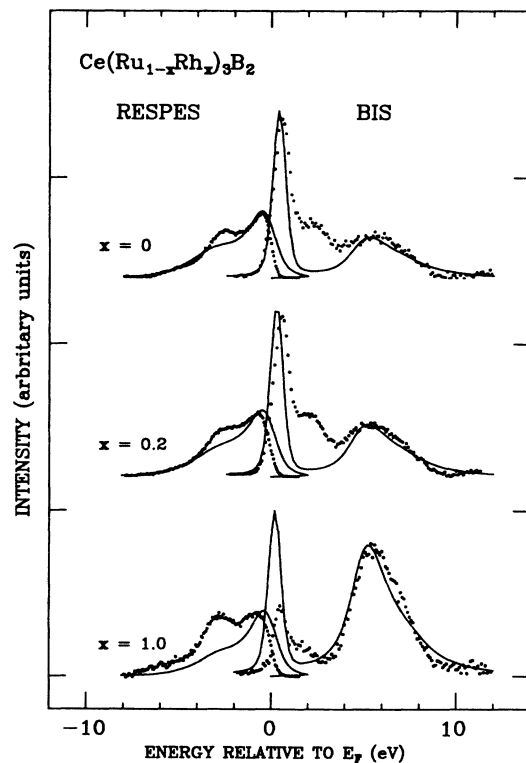

FIG. 9. The points and solid curves denote, respectively, the measured Ce $4f$ RESPES-BIS spectra and the corresponding theoretical fits of $Ce(Ru_{1-x}Rh_x)_3B_2$.
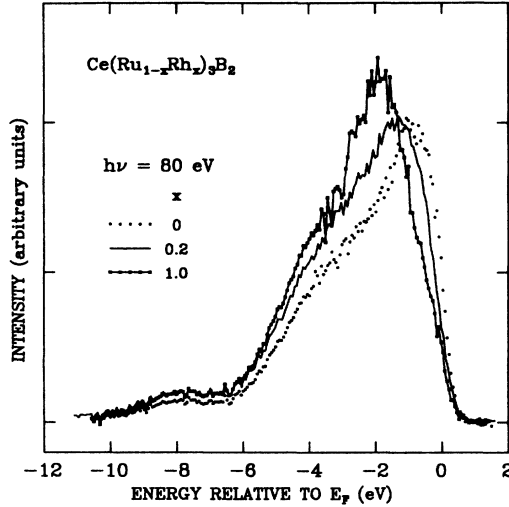
FIG. 10. Valence-band PES spectra for $Ce(Ru_{1-x}Rh_x)_3B_2$ compounds at $h\nu = 80$ eV, corrected as described in the text.

The spectra for $x = 0$ and 1 in Fig. 10 have been corrected to remove emission from grain-boundary carbon which occurs in the binding-energy range from 5 to 10 eV. In our previous publication[8] we assigned such carbon emission to the B $2s/2p$ states predicted for this energy range in band calculations.[21,22] However, the photoionization cross sections[20] for B $2s/2p$ are very small relative to that of other states in this photon-energy range, and the emission in this binding-energy region has intensity that varies considerably from sample to sample and from fracture to fracture. We have found that the samples where this emission is large in our RESPES studies have large carbon $1s$ emission in our subsequent XPS-BIS studies. That the emission is from interstitial and not bulk carbon is shown by the fact that for several fractures of the same sample, the appearances of the other valence-band features are independent of the strength of this emission, even when it is the largest. Since the sample for the $x = 0.2$ spectrum of Fig. 10 had a negligible carbon $1s$ XPS peak, we take this spectrum to show the intrinsic B s/p emission. The crystalline forms of carbon have extremely weak PES-BIS features in the range of ± 5 eV of E_F,[23] and so the interstitial carbon is not expected to influence our spectra in this range. Thus, our correction of the $x = 0$ and 1 spectra of Fig. 10 consists of smoothly replacing the emission in the region of the binding energy 10–5 eV by that of the $x = 0.2$ spectrum, assuming that the B s/p emission is not changing greatly with x.

For cerium materials, a coherent account of the $4f$ RESPES-BIS spectra, and of certain ground-state properties, has been obtained using the degenerate impurity Anderson Hamiltonian.[13,24−29] This Hamiltonian is a model for an N_f-fold degenerate local orbital hybridized to a band. It is characterized by parameters U_{ff}, ε_f, and $\rho N_f V^2$, which are, respectively, the Coulomb repulsion between two f electrons, the f binding energy relative to E_F, and the hybridization width involving hybridization

matrix element V of the f state to the conduction electrons having density of states ρ. The analysis done here uses the method of the $(1/N_f)$ expansion developed by Gunnarsson and Schönhammer[27] for this problem. It also includes the $4f$ spin-orbit splitting Δ_{so}, but not crystal-field splittings.

Of great importance, this model has a derived low-energy scale for spin fluctuations, called the Kondo temperature T_K. Insight into the model is gained from results to lowest order in $(1/N_f)$, with energy independent $\Delta = \pi \rho V^2$, and where U_{ff} is much larger than any other parameter. Then T_K depends exponentially on $(-1/J)$, where J is the Kondo coupling constant formed from the Hamiltonian parameters, roughly as $J = (N_f \Delta)/\pi \varepsilon_f$. Also, the occupation of the local orbital n_f is related to $\delta = k_B T_K$ as $n_f/(1-n_f) = N_f \Delta/\pi \delta$, so that small T_K occurs for n_f very near 1. Thermodynamic and ground-state properties such as the static dc magnetic susceptibility $\chi(0)$ and the T linear specific-heat coefficient γ are proportional to $(1/T_K)$. The $4f$ spectrum displays ionization and affinity peaks roughly at ε_f and $\varepsilon_f + U_{ff}$ in the RESPES and BIS spectra, respectively, and in addition a peak near E_F, called the Kondo resonance, whose position, width and weight are governed by T_K. In the BIS spectrum the peak is at δ and has integrated weight proportional to $N_f(1-n_f)$, so it is large only if T_K is relatively large. This peak can easily be seen in the BIS spectra of Fig. 9. In the photoemission spectrum the tail of the BIS peak produces a sharp rise in the region within δ of E_F. The spectra of Fig. 9 also show this feature, which includes extra weight[13] occurring when spin-orbit splitting and finite U_{ff} are included in the model.

It has also been possible[27] to describe the Ce $3d$ XPS spectrum by including in the Hamiltonian a term describing the attractive Coulomb interaction U_{fc} between the core hole and the $4f$ electron. In general, the $3d$ spectrum displays three peaks for each spin-orbit-split component, corresponding approximately to final states with different $4f$ valences. With reference to Fig. 8, the shoulder at lowest binding energy in the $3d$ spectrum is the $3d^9_{5/2}4f^2$ peak, the magnitude of which is controlled by Δ averaged over the valence band, Δ_{av}. For all x the peaks are large, indicating hybridization which is substantial, but decreasing slightly as x changes from 0 to 1. The highest binding-energy peak in the $3d$ spectrum, the $3d^9_{3/2}4f^0$ final state, gives a measure of $(1-n_f)$. This peak also decreases as x changes from 0 to 1, although it is never small. Its intensity correlates with that of the BIS peak near E_F.

For our theoretical analysis, the spectra shown in Fig. 10 are taken as an approximation of the energy dependence of Δ. The spectra are scaled relative to one another so that the area under each curve is proportional to the number of transition-metal $4d$ electrons. It is important that when Δ is energy dependent, J and the value of T_K depend primarily on Δ at E_F, $\Delta(E_F)$, so that the decrease in the conduction-band density of states at E_F as x changes from 0 to 1 is very significant. Thus, even though the hybridization matrix element V is of similar magnitude for both Ce-Rh and Ce-Ru hybridization, our

analysis shows that T_K is considerably reduced as x varies from 0 to 1, and $\Delta(E_F)$ decreases. The solid lines in Figs. 8 and 9 show, respectively, the theoretical fits for the Ce $3d$ and $4f$ spectra, using essentially the same parameter values for the two spectra. The quality of the fits is similar to that obtained previously for other intermetallic compounds of Ce with transition metals.[13] For $x=1$, we have fit the Ce $3d$ XPS spectrum and used these parameters to calculate the BIS spectrum. That the experimental intensity in the Kondo resonance is less than in the calculated spectrum reflects the slightly oxidized surface, which is more trivalent than would be the case for the intrinsic material.

Table II summarizes the information obtained from our fits for $Ce(Ru_{1-x}Rh_x)_3B_2$. The values of ε_f from the fits are about -1.4 eV for all x. The values of Δ_{av} are about 0.105, 0.10, and 0.095 eV for $x=0$, 0.2, and 1, respectively, indicating that V changes little with x. These parameters give, respectively, values of n_f of 0.76 (0.80), 0.78 (0.81), and 0.88 (0.91), for $x=0$, 0.2, and 1, and for the XPS-PES (BIS) fits. The values of n_f obtained from the Ce $3d$ XPS and $4f$ PES fits are slightly smaller than those obtained from BIS fits. The value of $n_f \approx 0.9$ for $x=1$ is in good agreement with the value reported by Kasaya *et al.*[12] We have also calculated the zero-temperature magnetic susceptibility $\chi(0)$ to lowest order in $(1/N_f)$, for the parameter values of the fits, and extracted a Kondo temperature defined by the relation $\chi(0)=Cn_f/T_K$, where $C=0.807$ emu K/mol is the Curie constant appropriate for the $J=\frac{5}{2}$ $4f^1$ state. The values of T_K are ~ 2500, ~ 1700, and ~ 400 K, for $x=0$, 0.2, and 1, respectively. For $x=0$, the value of the theoretical $\chi(0)$ is $\sim 0.25 \sim 10^{-3}$ emu/mol of the Ce atom, comparable to the experimental value of 0.6×10^{-3} emu/mol, shown in Fig. 6. If the experimental value of $\chi(0)$ for $LaRu_3B_2$, presently unknown, were subtracted from $\chi(0)$ for $CeRu_3B_2$ to find the contribution of the Ce $4f$ electron to the $\chi(0)$ in $CeRu_3B_2$, the result would be closer to the theoretical value. Our calculations do not include the

crystal-field splittings, which are thought to be the order of 100 K. For $x=0$ and 0.2, T_K is so large that this approximation should be reasonable. For $x=1$, where the calculated T_K may be only a few times larger than the crystal-field splitting, the neglect of the splitting may be more serious. However, our fit reproduces the intensity of the highest binding-energy peak of the $3d$ XPS spectrum, which is controlled by $(1-n_f)$. Since $(1-n_f)$ is also the dominant factor controlling the susceptibility, we expect that our calculated value of $\chi(0)$ is reasonably accurate. However, the value of the Curie constant C in our definition of T_K should be changed to reflect the crystal-field splittings, and its value depends in detail on the wave functions produced by the splittings, which are not presently known. In the absence of more detailed knowledge, we must accept some uncertainty in the value of T_K for $x=1$.

V. DISCUSSION

The phase diagram for $Ce(Ru_{1-x}Rh_x)_3B_2$, shown in Fig. 2, summarizes the experimental transport and magnetic results reported above. Superconductivity exists in the range $0<x<0.38$, while ferromagnetism occurs in the range $0.84<x<1.0$, with no region of overlap between the two phenomena. Our studies of superconductivity and ferromagnetism in $Ce(Ru_{1-x}Rh_x)_3B_2$ show that ferromagnetism is associated with nearly trivalent Ce ions, which are generally consistent with those of $(La_{1-x}Ce_x)Rh_3B_2$ and $Ce(Ru_{1-x}Rh_x)_3B_2$ reported by Shaheen *et al.*[10] The substitution of Ru for Rh in $CeRh_3B_2$ produces a very rapid depression of T_M, while the substitution of Rh for Ru in $CeRu_3B_2$ does not have a strong effect on superconductivity. These results show that the ferromagnetism in $CeRh_3B_2$ is rapidly destabilized by the substitution of Ru for Rh. The nonmonotonic variation of T_c with x can be attributed to two effects. The initial increase in T_c with x for $x<0.1$ is probably due to the increase in the average electron con-

TABLE II. Parameter values of $Ce(Ru_{1-x}Rh_x)_3B_2$, used for fitting the $3d$ XPS, $4f$ PES, and BIS spectra, and deduced values of the f occupancy n_f, the Kondo temperature T_K, and the static $T=0$ susceptibility $\chi(0)$.

| | $Ce(Ru_{1-x}Rh_x)_3B_2$ | | | | | |
| | $x=0$ | | $x=0.2$ | | $x=1$ | |
	PES-XPS	BIS	PES-XPS	BIS	PES-XPS	BIS
ε_{f0} (eV)	-1.4	-1.4	-1.4	-1.4	-1.4	-1.4
U_{ff} (eV)	6.6	6.0	6.4	6.2	6.6	6.6
U_{fc} (eV)	10.3		10.3		10.7	
f^0	0.281	0.254	0.260	0.239	0.157	0.135
f^1	0.677	0.688	0.701	0.711	0.808	0.822
f^2	0.042	0.058	0.039	0.050	0.035	0.043
n_f	0.76	0.80	0.78	0.81	0.88	0.91
Δ_{av} (eV)	0.109	0.104	0.102	0.100	0.095	0.095
$\Delta(E_F)$ (eV)	0.123	0.118	0.058	0.057	0.044	0.044
T_K (K)	~ 2450	~ 2280	~ 1740	~ 1540	~ 430	~ 380
$\chi(0)$ (10^{-3} emu/mol)	0.25	0.28	0.36	0.42	1.65	1.94

centration, while the decrease in T_c with x for $x > 0.1$ is presumably at least partially due to the approach of the ferromagnetic instability. We interpret, in the discussion below, the rapid decrease of T_M with decreasing x as due to a sharp increase in T_K.

For $CeRu_3B_2$, all our spectra are typical of materials having large hybridization, $n_f \sim 0.8$, and a very large Kondo temperature. The $3d$ spectrum of $CeRh_3B_2$ also shows rather large hybridization, but with n_f somewhat closer to 1. Table II shows that as x changes from 0 to 1 the values of ε_f, U_{ff}, and Δ_{av} do not change much. In contrast, the value of T_K changes dramatically as x changes from 0 to 1. For x near 0 the values of T_K are much larger than T_c, whereas for $x = 1$, T_K has decreased and is comparable to T_M. The decrease of T_K with x is mostly due to the change in $\Delta(E_F)$, which decreases by percentages that are 5–10 times larger than the percentage changes in Δ_{av} as x varies from 0 to 1. The change of T_K and $\Delta(E_F)$ also correlates with the transition with x from superconductivity to magnetism. We will argue below that this correlation is not coincidental, and so we conclude that the controlling variation in this alloy system is the transition metal $4d$ density of states of E_F. Such a mechanism was proposed previously for $CeIn_{3-x}Sn_x$ on nonspectroscopic grounds.[30,31]

The ferromagnetism of $CeRh_3B_2$ has been a continuing object of study and speculation. The reduced value of μ_s and the high value of T_M led Dhar et al.,[2] who first reported the ferromagnetism, to propose that it is probably itinerant in nature and associated with the Rh $4d$ electrons. However, this idea has been abandoned because RESPES data[8,11] show a small density of Rh $4d$ states at E_F, and because the neighboring $LaRh_3B_2$ compound does not exhibit ferromagnetism and is even superconducting with critical temperature $T_c = 2.5$ K, in spite of the fact that RRh_3B_2 compounds ($R =$ La, Ce, and Pr) have essentially identical Rh $4d$ bands.[11] Considering the Ce $4f$ electrons, it might seem that the ferromagnetism, high Curie temperature, and reduced values of μ_s and μ_{eff} compared with Ce^{3+} free-ion values would be naturally explained in terms of an itinerant model, i.e., a $4f$ band. However, by the end of 1985 considerable evidence had accumulated against such a picture, at least in its simplest form. L_{III}-edge x-ray-absorption spectroscopy (XAS) measurements[11,15] gave a Ce valence close to $3+$, RESPES measurements[8,11] found a $4f$ spectrum known[29] at that time to be typical for Ce in the Kondo regime of the Anderson Hamiltonian, and NMR measurements[6,7] found that the magnetic moment is considerably localized at the Ce site below T_M and that the spin fluctuations above T_M behave as a localized moment. Further, studies of the alloy system $(La_{1-x}Ce_x)Rh_3B_2$ revealed[10] a very rapid initial suppression of the T_c of $LaRh_3B_2$, ~ -5.6 K/at. % Ce substitution for La, and a small depression of the T_M of $CeRh_3B_2$, ~ -1.4 K/at. % La substitution for Ce. These alloy results, and those for $Ce(Ru_{1-x}Rh_x)_3B_2$, reported previously[8–10] and herein, can be interpreted in terms of well-defined localized magnetic moments on nearly trivalent Ce ions. Subsequent work on other alloy systems[32,35] has not altered this basic conclusion. Also,

band-structure calculations[21,22] done for $LaRh_3B_2$ and $CeRh_3B_2$ yield calculated values of γ similar to experiment for the La compound but not for the Ce compound, suggesting strong electronic correlations for the $4f$ electrons.

Models for the ferromagnetism that are based on localized moments of nearly trivalent Ce ions are immediately confronted by the need to account for the reduced value of the moments and the high value of T_M. Attention is naturally drawn to the highly anisotropic hexagonal crystal structure, but it appears that the reduced moment cannot be explained simply by the crystal-field splitting of the $J = \frac{5}{2}$ state into three doublets.[6,7] Shaheen et al.[10] concluded that the ferromagnetism and high T_M are associated with strong anisotropic hybridization of localized $4f$ electrons with conduction electrons, i.e., hybridization primarily in the direction of the hexagonal c axis along which the Ce interatomic spacing is unusually small. The reduced magnetic moment was then attributed to a Kondo-type compensation of the Ce localized moment arising from hybridization to the conduction electrons. Malik et al.[15] also suggested that the reduced moment may be a consequence of a Kondo-type interaction coupled with crystal-field effects. We have proposed[8] that the natural scenario for incorporating the Kondo effect in a ferromagnetic state is that of an exchange-split Kondo resonance, and we return to this idea at the end of this section.

Other ideas that do not involve the Kondo effect in the ferromagnetic state have been put forth. Kasuya and his co-workers have proposed[22,36,37] a model where the ferromagnetic state is caused by a crossover from a dense Kondo state at high temperature to an exchange-split band state at low temperature. Based on a conventional band calculation[22] the important band is identified as one based on an f orbital with quenched angular momentum, associated with the lowest crystal-field level. It has a rather one-dimensional character, with relatively large dispersion from direct $4f/4f$ mixing along the c axis. It might be expected that such a band would be more drastically affected by La or Gd substitutions than is implied by the alloy results cited above, but Kasuya argues qualitatively that this is not the case. The detailed quantitative theory of this complex model is still evolving, and it is not yet straightforward to assess its predictions against all the available data. It is argued that recent single-crystal studies support the model. Attention is called especially to the interpretation of neutron-scattering data[37] in which the magnetic moments on the Ce site and Rh site were assigned as 0.84 and $-0.09\mu_B$, respectively, implying a moment of $0.57\mu_B$/mol, somewhat larger than the saturation moment cited above. Finally, from a study of the magnetic properties of the isostructural compounds RRh_3B_2 ($R =$ La, Ce, Nd, Gd), Takeda et al.[38] conjectured the existence of a weak antiferromagnetic interaction between the R ions on neighboring ferromagnetic c-axis chains, and suggested that this could help explain the reduced moments.

We return now to the scenario of an exchange-split Kondo resonance, proposed by us in 1985. This picture could also be described by saying that the ferromagnetic

state is a band ferromagnet built from the quasiparticles of a Kondo Fermi liquid, associated with a Kondo resonance having the coherence[39] of the crystal's translational symmetry. It is analogous to the explanation given for the occurrence of superconductivity in materials containing nearly trivalent Ce, such as $CeCu_2Si_2$,[40] $CeRu_2$,[41] $CeCo_2$,[41] and the material studied here, $CeRu_3B_2$. The magnetic moment of the Ce, which nearly always suppresses T_c when Ce is an impurity in a superconducting host, is quenched coherently by formation of a nonmagnetic Kondo Fermi-liquid state at higher temperature, allowing a superconducting state to form by pairing the resulting quasiparticles. Considering our alloy results here, it is natural to think in terms of competition between superconducting and magnetic states of this Fermi liquid. The enhanced γ value of $CeRh_3B_2$ is consistent with the existence of such a Kondo Fermi liquid. Essentially then, the exchange-split Kondo resonance is an ansatz for a possible ground state of the Anderson lattice Hamiltonian. In our opinion the preponderance of the available evidence, and experience with other cerium materials[13] supports the choice of this Hamiltonian to model the system.

Recent theory has been directed at a ferromagnetic state of the kind we have proposed, and connections to our spectroscopic results can be made, as we now describe. Cox[42] has given an application of the molecular-field theory of magnetic ordering to the Anderson lattice model. In this treatment when the molecular-field exchange strength is comparable to the Kondo temperature, ferromagnetic order can occur with a behavior reminiscent of itinerant magnetism. In particular, the magnitude of the magnetic moment is noninteger. We have previously pointed out[8] that merely invoking strong hybridization and the anisotropic crystal structure, as done in several of the qualitative pictures, is insufficient to understand why $CeRh_3B_2$ is so unusual. All cerium intermetallics studied thus far[13] display hybridization between the $4f$ and conduction electrons, and this hybridization is frequently strong. In the alloy series discussed in this paper, the anisotropic crystal structure is maintained for all x, the average hybridization is even larger for $x=0$ than for $x=1$, and yet the $x=0$ compound has much different ground-state properties. Our spectroscopic results show that the factor not identified in previous work is the variation in the density of the transition-metal d states at E_F. The different properties of $CeRu_3B_2$ result from its very large value of T_K, which is, in turn, enabled by the large density of Ru d states at E_F. An equally large T_K is frustrated in the Rh compound by the decreased density of Rh d states at E_F. We hypothesize here that the origin of the strong ferromagnetic exchange interaction is indeed the strong hybridization, but that it should be understood as a kind of superexchange interaction, analogous to that in an insulator. That is, the Rh d band, which is mostly below E_F, plays much the same role as does the filled oxygen band in a magnetic metal-oxide insulator. Such an interaction will involve not the value of Δ at E_F, $\Delta(E_F)$, as for the Ruderman-Kittel-Kasuya-Yosida (RKKY) interaction and the Kondo effect, but rather its average value Δ_{av}. Thus, one can

have a large exchange interaction in the Rh compound while keeping the value of T_K small enough to meet the condition for ferromagnetism.

Spectroscopic consequences of this scenario are expected. Gunnarsson and Schönhammer[27] have considered the effect of a molecular field in the impurity Anderson model and found that the Kondo resonance persists, but that the weight is pushed away from E_F by the energy stablization of the magnetic state. Direct observation of this exchange splitting will require much better resolution than was employed in the studies reported here. More recently Jo and Imada[43] have used a similar molecular-field model to calculate the Ce $4d$ x-ray-absorption spectrum. They include multiplet splittings of the absorption final state and predict strong circular dichroism in the spectrum. It seems likely that additional spectroscopic studies of this kind can be used to test the Anderson lattice picture of the ferromagnetism of $CeRh_3B_2$.

It would be naive to suppose that our discussion here has identified all the factors which bring about ferromagnetism in $CeRh_3B_2$. We are, after all, using an impurity theory which includes the lattice only in an average way. Other details of the electronic structure and the geometry of the lattice must be important in determining such things as the sign of the magnetic exchange interaction. Another interesting issue is that transport data[12] for Ce dilutely present in $LaRh_3B_2$ suggests $T_K \sim 5$ K, much smaller than the T_K we have estimated spectroscopically for $CeRh_3B_2$, and not compatible with our model in being much smaller than T_M. Kasuya[12] assumes that the small T_K persists as La is entirely replaced by Ce to form $CeRh_3B_2$. However, the lanthanide contraction, and experience with other materials, suggests that La may increase the average volume, decreasing V and decreasing T_K exponentially in V^2. Spectroscopic studies of the La-Ce alloy would be required to settle this question. While there remain such uncertainties and a lack of detailed knowledge of all the important factors, we believe we have identified the preconditions that must be met for the occurrence of ferromagnetism in $CeRh_3B_2$.

VI. SUMMARY

Our studies of superconductivity and ferromagnetism in $Ce(Ru_{1-x}Rh_x)_3B_2$ show that ferromagnetism is associated with nearly trivalent Ce ions. The analysis of electron spectroscopy data for $Ce(Ru_{1-x}Rh_x)_3B_2$ using the impurity Anderson Hamiltonian, enables the direct identification of the alloying mechanism controlling the low-energy properties of this alloy system. We find that the controlling variation is not in any parameter directly connected to the $4f$ states, but is in the transition-metal $4d$ density of states at the Fermi level. The fact that the average hybridization in $CeRh_3B_2$ is very large, and that a large T_K is only avoided because the density of Rh d states at E_F is small allows us to understand how hybridization can bring about a large exchange interaction without producing an equally large Kondo effect that would otherwise suppress the magnetic state. This situation is then favorable to bring about a ferromagnetic state

based on the Kondo Fermi liquid, i.e., the exchange-split Kondo resonance we have previously proposed for rationalizing the localized and itinerant aspects of the ferromagnetism of this unusual material.

ACKNOWLEDGMENTS

*Also at the Department of Physics, University of Michigan, Ann Arbor, Michigan 48109-1120.

[1] K. N. Yang, M. S. Torikachvili, M. B. Maple, and H. C. Ku, J. Low Temp. Phys. **56**, 601 (1984).

[2] S. K. Dhar, S. M. Malik, and R. Vijayaraghavan, J. Phys. C **14**, L321 (1981).

[3] H. C. Ku, G. P. Meisner, F. Acker, and D. C. Johnston, Solid State Commun. **35**, 91 (1980).

[4] K. N. R. Taylor, Adv. Phys. **20**, 551 (1971).

[5] S. K. Malik, S. K. Dhar, and R. Vijayaraghavan, J. Appl. Phys. **53**, 8074 (1982).

[6] Y. Kitaoka, Y. Kishimoto, K. Asayama, T. Kohara, K. Takeda, R. Vijayaraghvan, S. K. Malik, S. K. Dhar, and D. Rambabu, J. Magn. Magn. Mater. **52**, 449 (1985).

[7] R. Vijayaraghvan, J. Magn. Magn. Mater. **52**, 37 (1985).

[8] M. B. Maple, S. E. Lambert, M. S. Torikachvili, K. N. Yang, J. W. Allen, B. B. Pate, and I. Lindau, J. Less Common Met. **111**, 239 (1985).

[9] K. N. Yang, Ph.D. thesis, University of California at San Diego, 1985.

[10] S. A. Shaheen, J. S. Schilling, and R. N. Shelton, Phys. Rev. B **31**, 656 (1985).

[11] E. V. Sampathkumaran, G. Kaindl, C. Laubschat, W. Krone, and G. Wortmann, Phys. Rev. B **31**, 3185 (1985).

[12] M. Kasaya, A. Okabe, T. Takahashi, T. Satoh, T. Kasuya, and A. Fujimori, J. Magn. Magn. Mater. **76&77**, 347 (1988).

[13] J. W. Allen, S.-J. Oh, O. Gunnarsson, K. Schönhammer, M. B. Maple, M. S. Torikachvili, and I. Lindau, Adv. Phys. **35**, 175 (1986).

[14] See, for example, S. Roth, Appl. Phys. **15**, 1 (1978).

[15] S. K. Malik, A. M. Umarji, G. K. Shenoy, P. A. Montano, and M. E. Reeves, Phys. Rev. B **31**, 4728 (1985).

[16] K. N. Yang, M. S. Torikachvili, M. B. Maple, and H. C. Ku, J. Appl. Phys. **57**, 3140 (1985).

[17] F. U. Hillebrecht, J. C. Fuggle, G. A. Sawatzky, and R. Zeller, Phys. Rev. Lett. **51**, 1187 (1983).

[18] U. Fano, Phys. Rev. **124**, 1866 (1961).

[19] G. Rossi, I. Lindau, L. Braicovitch, and I. Abatti, Phys. Rev. B **28**, 2362 (1982).

[20] J. J. Yeh and I. Lindau, At. Data Nucl. Tables **32**, 1 (1985).

[21] D. K. Misemer, S. Auluck, S. I. Kobayashi, and B. N. Harmon, Solid State Commun. **52**, 955 (1984).

[22] K. Takegahara, H. Harima, and T. Kasuya, J. Phys. Soc. Jpn. **54**, 4743 (1985).

[23] B. B. Pate, Ph.D. thesis, Stanford University, 1985.

[24] J. W. Allen, S.-J. Oh, I. Lindau, J. M. Lawrence, L. I. Johansson, and S. B. Hägstrom, Phys. Rev. Lett. **46**, 1100 (1981).

[25] M. Croft, J. H. Weaver, D. J. Peterman, and A. Franciosi, Phys. Rev. Lett. **46**, 1104 (1981).

[26] J. W. Allen and R. M. Martin, Phys. Rev. Lett. **49**, 1106 (1982).

[27] O. Gunnarsson and K. Schönhammer, Phys. Rev. Lett. **50**, 604 (1983); Phys. Rev. B **28**, 4315 (1983); **31**, 4815 (1985); in Handbook on the Physics and Chemistry of Rare Earths, edited by K. A. Gschneidner, L. Eyring, and S. Hüfner (North-Holland, Amsterdam, 1987), Vol. 10, p. 103.

[28] J. W. Allen, S.-J. Oh, M. B. Maple, and M. S. Torikachvili, Phys Rev. B **28**, 5347 (1983).

[29] J. W. Allen, J. Less Common Met. **93**, 183 (1983).

[30] J. M. Lawrence and D. Murphy, Phys. Rev. Lett. **40**, 961 (1978).

[31] J. M. Lawrence, Phys. Rev. B **20**, 3770 (1979).

[32] S. K. Dhar and S. K. Malik, in Theoretical and Experimental Aspects of Valence Fluctuations and Heavy Fermions, edited by L. C. Gupta and S. K. Malik (Plenum, New York, 1987), p. 467.

[33] A. M. Umarji and S. K. Malik, in Theoretical and Experimental Aspects of Valence Fluctuations and Heavy Fermions, Ref. 32, p. 471.

[34] A. K. Grover and S. K. Dhar, in Theoretical and Experimental Aspects of Valence Fluctuations and Heavy Fermions, Ref. 32, p. 481.

[35] S. K. Malik, G. K. Shenoy, S. K. Dhar, P. L. Paulouse, and R. Vijayaraghavan, Phys. Rev. B **34**, 8196 (1986).

[36] T. Kasuya, M. Kasaya, K. Takegahara, F. Iga, B. Liu, and N. Kobayashi, J. Less Common Met. **127**, 337 (1987).

[37] T. Kasuya, K. Takegahara, N. Kobayashi, M. Kasaya, and A. Okabe, in Theoretical and Experimental Aspects of Valence Fluctuations and Heavy Fermions, Ref. 32, p. 187.

[38] K. Takeda, T. Kohara, Y. Kitaoka, and A. Asayama, Solid State Commun. **62**, 711 (1987).

[39] R. M. Martin, Phys. Rev. Lett. **48**, 362 (1982).

[40] F. Steglich, C. D. Bredl, W. Lieke, U. Rauchschwalbe, and G. Sparn, Physica B+C **126B**, 82 (1984).

[41] J. W. Allen, S.-J. Oh, I. Lindau, M. B. Maple, J.-F. Suassuna, and S. B. Hagström, Phys. Rev. B **26**, 445 (1982).

[42] D. L. Cox, Phys. Rev. B **35**, 4561 (1987).

[43] T. Jo and S. Imada, J. Phys. Soc. Jpn. **58**, 1922 (1989).